Modeling the Effects of UV Variability and the QBO on the Troposphere–Stratosphere System. Part II: The Troposphere

DAVID RIND* AND NAMBATH K. BALACHANDRAN

Columbia University, Global Systems Institute, New York, New York

(Manuscript received 23 June 1994, in final form 8 March 1995)

ABSTRACT

Results of experiments with a GCM involving changes in UV input (±25%, ±5% at wavelengths below 0.3 μ) and simulated equatorial QBO are presented, with emphasis on the tropospheric response. The QBO and UV changes alter the temperature in the lower stratosphere/upper troposphere, affecting tropospheric/stratospheric vertical stability. When the extratropical lower stratosphere/upper troposphere warms, tropospheric eddy energy is reduced, leading to extratropical tropospheric cooling of some 0.5°C on the zonal average, and surface temperature changes up to ±5°C locally. Opposite effects occur when the extratropical lower stratosphere/upper troposphere cools. Cooling or warming of the comparable region in the Tropics decreases/increases static stability, accelerating/decelerating the Hadley circulation. Tropospheric dynamical changes are on the order of 5%.

The combined UV/QBO effect in the troposphere results from its impact on the middle atmosphere: in the QBO east phase, more energy is refracted to higher latitudes, due to the increased horizontal shear of the zonal wind, but with increased UV, this energy propagates preferentially out of the polar lower stratosphere, in response to the increased vertical shear of the zonal winds; therefore, it is less effective in warming the polar lower stratosphere. Due to their impacts on planetary wave *generation* and *propagation*, all combinations of UV and QBO phases affect the longitudinal patterns of tropospheric temperatures and geopotential heights. The modeled perturbations often agree qualitatively with observations and are of generally similar orders of magnitude.

The results are sensitive to the forcing employed. In particular, the nature of the tropospheric response depends upon the magnitude (and presumably wavelength) of the solar irradiance perturbation. The results of the smaller UV variations (±5%) are more in agreement with observations, showing clear differences between the UV impact in the east and west QBO phase. However, since the UV magnitudes have been exaggerated relative to observed solar UV variations during the last solar cycle, the results cannot be used to prove an actual solar forcing of the troposphere. The results will also likely be sensitive to the model, particularly its planetary longwave energy, and may be influenced by other processes that have not been included, such as changes in stratospheric ozone.

The dynamical changes are accompanied by changes in cloud cover and snow cover that differ between maximum and minimum UV, and affect the radiative balance of the planet. As these influences do not cancel in the extreme phases of the UV variations, a net radiative forcing may result from solar cycling in conjunction with the QBO. An assessment of the solar impact on climate change must include these dynamically driven forcings.

1. Introduction

In Part I of this study, we described the response of the middle atmosphere to a combination of the quasi-biennial oscillation (QBO) and variations in ultraviolet (UV) radiation (short of 0.3 μm). It was shown that both types of perturbations affect the refraction of atmospheric waves by altering wind gradients, primarily horizontal in the case of the QBO, and primarily vertical in the case of varying UV. It was also noted that since the results are sensitive to the precise perturbation involved, any comparison with observations should ultimately be done with the most accurate specification of the forcing. However, certain aspects of the study seem robust; in particular, the QBO in both the model and observations results in a quadrupole structure to the altitude/latitude temperature change response between the two phases. In contrast, the magnitude (and undoubtedly the wavelength) of the UV forcing appears to be of crucial importance in determining the response in the middle atmosphere, although the results for a particular magnitude of UV forcing also appear robust over 10 years of integration.

* Additional affiliation: NASA/Goddard Institute for Space Studies, New York, New York.

Corresponding author address: Dr. David Rind, NASA/GISS, 2880 Broadway, New York, NY 10025.
E-mail: cddhr@nasaglss.giss.nasa.gov

The most intriguing and practical aspect of the Labitzke–van Loon (LvL) studies (Labitzke and van Loon 1988, 1989; van Loon and Labitzke 1988) concerns the tropospheric response. Peak effects of a correlation between surface atmospheric temperatures and the solar cycle as modulated by the phase of the QBO "explain" some 50% of the variance for North Carolina temperatures in January and February. With correlations this high, Barnston and Livezey (1989) noted that they "justify immediate use for operational purposes" by the Climate Analysis Center. It is also this aspect of the work that has received the most skeptical response, given the orders of magnitude mismatch between the energy of tropospheric phenomena and that associated with solar variations.

Several modeling studies have already explored the influence of changes in stratospheric winds on the upward propagation of tropospheric planetary scale waves, associated with ozone and other perturbations, (Boville 1984, 1993; Kodera et al. 1990; Kodera 1993). In addition, observational studies have related anthropogenic trends in stratospheric circulation resulting from ozone depletion to alterations in the amplitudes and phases of stationary tropospheric waves in winter (Kodera and Yamazaki 1994; Hood and Zaff 1995). None of these results is definitive, as the GCM sensitivity to the given (often exaggerated) forcing is untested, and the observations tend to be limited to a few solar cycles at best.

Similarly, with the crudeness of the forcings used in these experiments and the inaccuracies in the model we cannot expect this study to prove or disprove the ability of solar variability to influence tropospheric processes. What we can do is explore the mechanisms with which the model responds to the given UV forcing, in the hope that this may provide indications of how the real world might respond.

An additional topic of interest concerns the ability of solar cycle irradiance variations to affect the global climate. Studies such as those of Friis-Christensen and Lassen (1991) suggest a relationship between solar variability and climate, but the magnitudes of the apparent changes in solar forcing required have not been directly observed. While this study is not designed to look at long-term climate changes, the results raise several relevant issues, which will be addressed in the discussion section.

The experiments discussed are those that were introduced in Part I, using the GISS Global Climate/Middle Atmosphere Model (Rind et al. 1988a,b). We will employ the same terminology; that is, +25W is 25% UV increase associated with west wind QBO phase, where −5E represents a 5% UV decrease with the east wind QBO phase, etc. Since the most obvious correlations are in the Northern Hemisphere during winter, the results described below will have this focus, unless otherwise indicated.

2. The QBO and the tropospheric response

How does the model-imposed QBO affect the troposphere? The temperature differences in four different sets of simulations, [+25E minus +25W], [−25E minus −25W], [+5E minus −5E], and [+5W minus −5W] for December through February are shown in Fig. 1. Associated with the east wind phase of the tropical QBO, the lower stratosphere/upper troposphere is relatively cool in the Tropics, and warm in the extratropics. In Part I it was noted that the extratropical impact was the result of a change in planetary wave propagation due to the altered horizontal wind gradient.

In the troposphere, all four sets of experimental differences show cooling in the extratropical lower and middle troposphere. With increased UV (top figures), the lower stratosphere/upper troposphere warming occurs more at midlatitudes, as does the low and middle tropospheric cooling. With decreased UV (bottom figures), the lower stratosphere/upper troposphere warming is more at higher latitudes, as is the low and middle tropospheric cooling. As discussed in Part I, the increased UV leads to a positive shear of the zonal wind in the stratosphere, and increased vertical energy propagation away from the polar lower stratosphere; this limits the QBO east phase warming at the highest latitudes. From Fig. 1, it is apparent that this distinction has an effect in the troposphere as well.

All four sets of differences are characterized by a general decrease in eddy kinetic energy in the extratropical troposphere (Fig. 2), with changes generally of the order of 5%–10%. The differences seen in the troposphere also occur through most of the stratosphere. This continuity is associated with a decrease in upward energy propagation, an effect that extends from the lower troposphere upward through much of the middle atmosphere at midlatitudes, although relative wave energy flux convergences are producing warming in the lower stratosphere. Once again some differences arise depending upon whether UV is increased or decreased: with increased UV (top figures), the energy decrease, like the lower stratosphere/upper troposphere warming, is more at middle latitudes; while with decreased UV, the energy decrease, and the lower stratosphere/upper troposphere warming, is more at high latitudes.

In conjunction with the reduced eddy energy there are reduced eddy transports at midlatitudes of moist static energy (Fig. 3), again often on the order of 5%–10%. The effect again depends upon the sign of the UV change, being larger with decreased UV (bottom figures) which featured larger and more consistent eddy energy changes. The weaker transports then lead to extratropical dynamical cooling (Fig. 4), hence explaining much of the colder temperatures seen there in Fig. 1. In the reduced UV experiments, the greater transport reductions lead to widespread dynamical

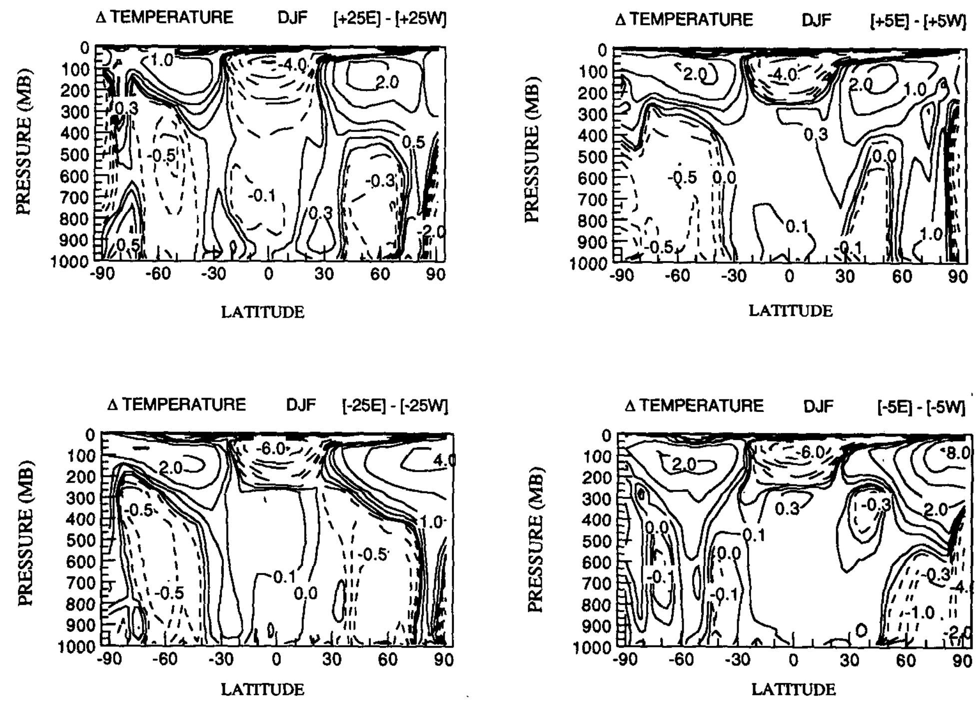

FIG. 1. Composite average model temperature difference (°C) for December through February between east and west phases of QBO: [+25 E] minus [+25W] (top left); [−25E] minus [−25W] (bottom left); [+5E] minus [+5W] (top right); and [−5E] minus [−5W] (bottom right). All results are averages over 3 years of each model simulation.

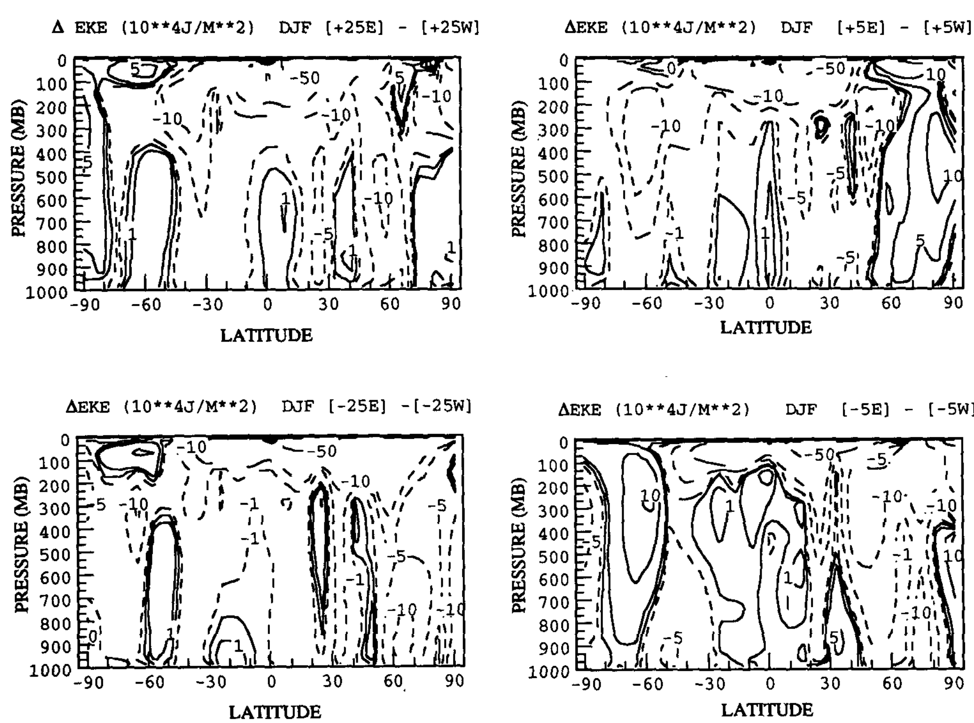

FIG. 2. As in Fig. 1 except for difference in eddy kinetic energy.

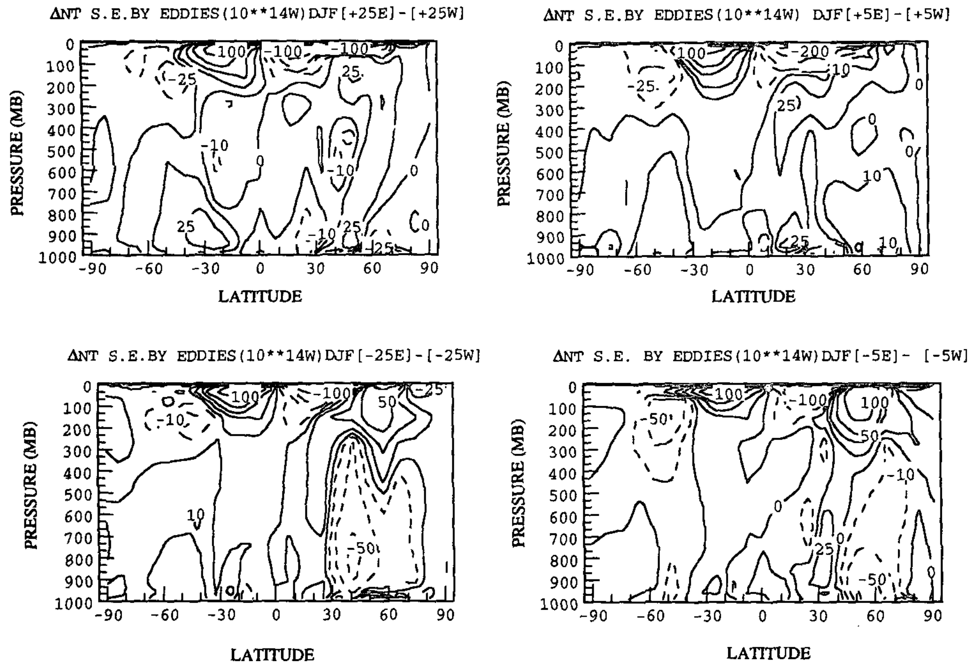

FIG. 3. As in Fig. 1 except for difference in eddy northward transport of moist static energy (the sum of sensible heat, latent heat, and geopotential energy). Note that positive values in the Southern Hemisphere indicate decreased poleward transport.

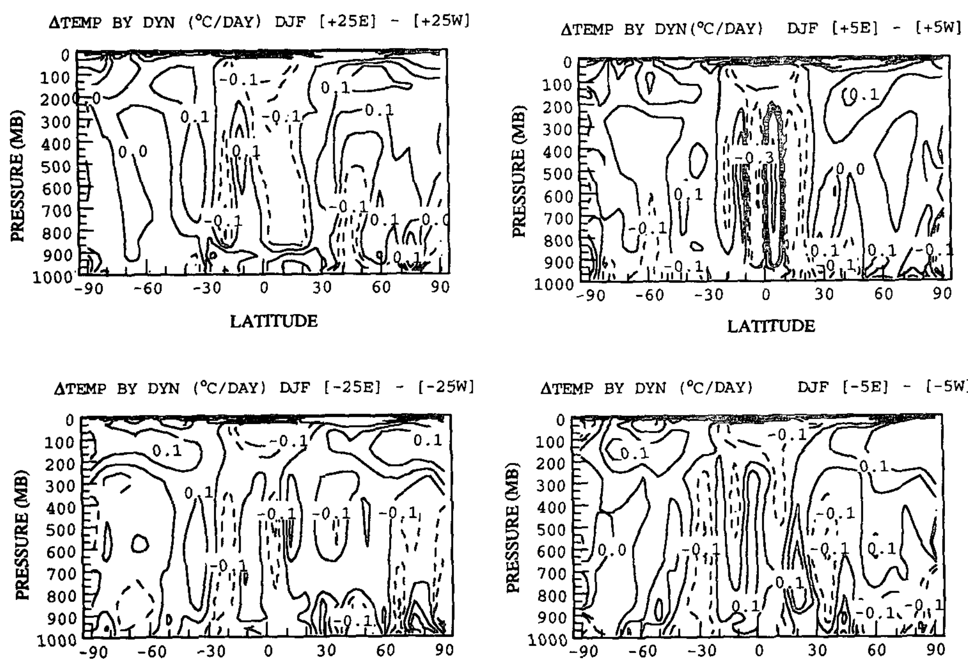

FIG. 4. As in Fig. 1 except for difference in the temperature change by dynamics.

cooling poleward of ~30°N, matching the temperature reductions, while with increased UV, the effects are confined to narrower midlatitude bands. Therefore, the low and midtropospheric cooling results from tropospheric dynamical changes, in particular, reduced eddy energy and eddy energy transports.

Why is the eddy energy lower with the east wind phase of the QBO? As indicated in Fig. 1, the tropical east wind change is associated with extratropical warming of the lower stratosphere and upper troposphere. In previous experiments with this model, changes in the lower stratosphere have been shown to influence the tropospheric dynamical response, primarily through the impact on vertical stability. For example, in the modeled doubled CO_2 climate, colder stratospheric temperatures (hence decreased vertical stability) led to greater long-wave available potential energy, and greater long-wave energy (Rind et al. 1990). In the experiment with increased volcanic aerosols, warming of the lower stratosphere was associated with greater stability and a reduction in the Hadley circulation (Rind et al. 1992). In the experiments discussed here, the warming of the extratropical lower stratosphere and upper troposphere is associated with increased stability and reduced eddy energy. Note that the effect on eddy energy is entirely due to an alteration in the vertical temperature gradient; the increase in latitudinal temperature gradient associated with reduced UV in the QBO experiments (Fig. 1, bottom) would have favored increased eddy energy. The relevant dynamical changes are summarized in Table 1.

There are low-latitude effects apparent in the troposphere as well. The cooling of the tropical lower stratosphere due to forcing in the QBO east phase decreases the vertical stability, and there is a corresponding increase in Hadley cell intensity in the Northern Hemisphere. This is most clearly seen in Fig. 4, which includes dynamical changes due to alterations in the mean circulation. In all the experiments there is a narrow region of cooling near the equator, due to increased vertical ascent, and often bands of warming on either side due to increased subsidence. Changes in the vertical motion field affect cloud cover, with increases in regions of rising air, and decreases with subsidence drying. The relevant tropospheric dynamical and cloud cover changes are also indicated in Table 1.

3. UV variability and tropospheric response

The average winter temperature differences (December through February) are presented in Fig. 5 for [+25W minus −25W], and [+25E minus −25E], [+5W minus −5W], and [+5E minus −5E], respectively. The outstanding feature of the increased UV experiments is the warming that occurs throughout most of the middle atmosphere. In the lower stratosphere/upper troposphere, the general response is for cooling in the Northern Hemisphere extratropics except in [+5W minus −5W], which features substantial warming.

The response for the lower and middle troposphere is once again generally of the opposite sign, especially in the extratropics: where there is cooling in the lower stratosphere/upper troposphere, there is warming below, and with warming in the lower stratosphere/upper troposphere, there is cooling below. Note, for example, the change in sign of tropospheric response in the 5% experiments for the east and west phases, which have opposite stratospheric responses. The results shown for the altered UV experiments in Fig. 5 are similar to those for the QBO experiments (Fig. 1), and the explanation is also similar. Eddy energy increases at higher latitudes (Fig. 6) in association with the reduced vertical stability except in [+5W] − [−5W] where the increased stability leads to eddy energy decreases. Where the eddy energy changes, so does the eddy energy transport (Fig. 7), hence [+5W] − [−5W] produces decreased eddy energy transport at higher latitudes, while the other experiments show increases. The dynamical temperature changes (Fig. 8), although affected by the mean circulation as well, maintain the character of the eddy energy transport effect, with high latitude warming in all the experiments except [+5W] − [−5W], which shows cooling. A comparison of Figs. 5 and 8 verify that the pattern of the actual temperature

TABLE 1. Tropospheric (1000–200 mb) changes in QBO experiments, for the months of December through February for 40°–90°N (except 30°–60°N for +5[E–W]), and in the Tropics.

	Parameter			
	+25[E–W]	−25[E–W]	+5[E–W]	−5[E–W]
Δtemperature(°C)	−0.2	−0.5	−0.1	−0.2
Δstatic stability (%)	3.8	5.6	4.3	5.2
ΔEKE (%)	−3.5	−4.3	−3.8	−6.0
Δnorthward eddy transport of energy (%) (NH)	0.0	−1.6	−3.4	−4.6
Δtemperature (68 mb) (10°S–15°N)	−5.5	−6.1	−5.6	−6.3
ΔHadley cell (%)	3.1	5.3	6.0	2.9
Δcloud cover (absolute %) (10°S–15°N)	2.2	2.5	1.6	2.3

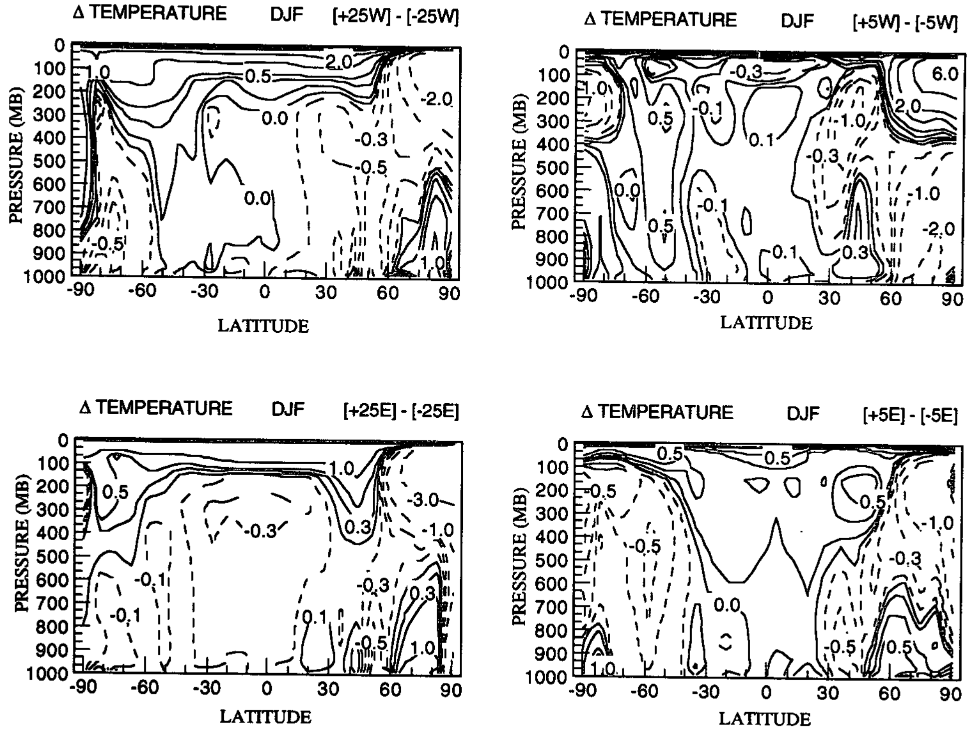

FIG. 5. Composite average model temperature difference (°C) for December through February between increased and decreased solar UV values: [+25W] minus [−25W] (upper left); [+25E] minus [−25E] (bottom left); [+5W] minus [−5W] (upper right); and [+5E] minus [−5E] (lower right).

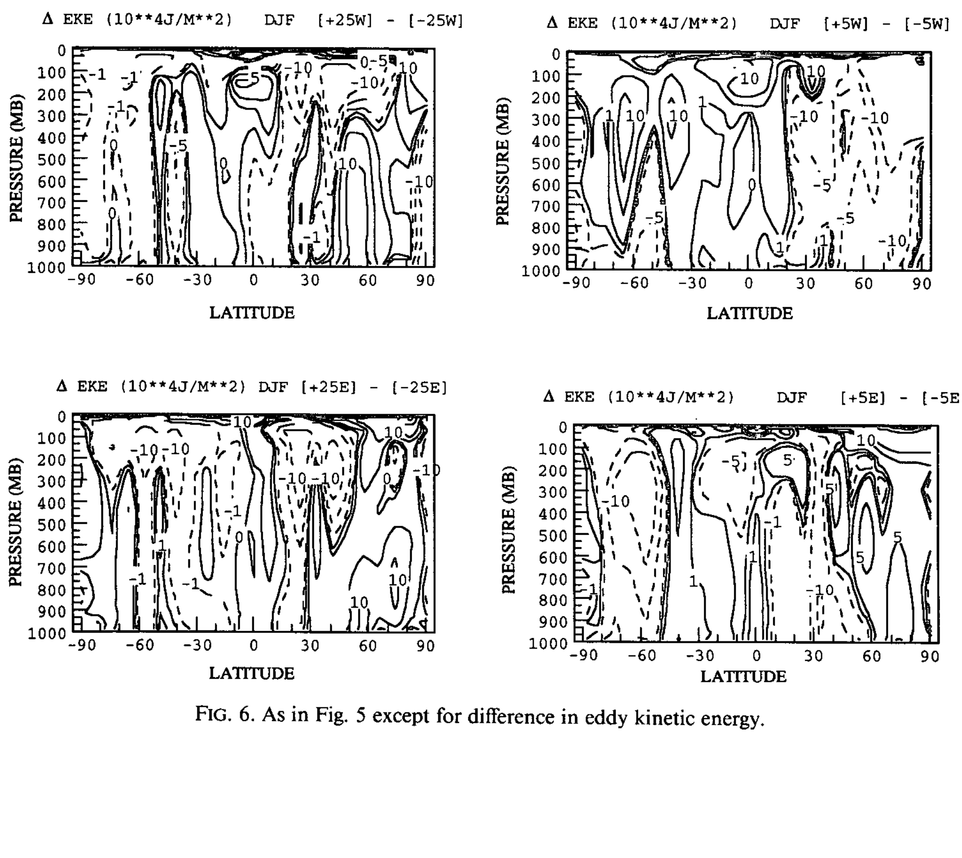

FIG. 6. As in Fig. 5 except for difference in eddy kinetic energy.

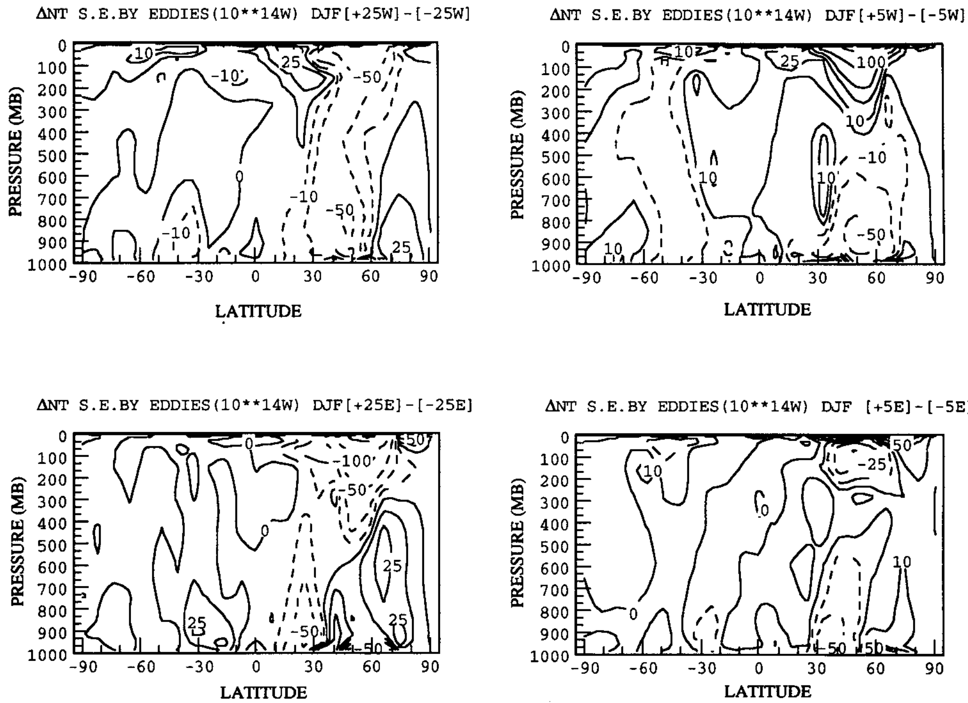

FIG. 7. As in Fig. 5 except for difference in eddy transport of moist static energy.

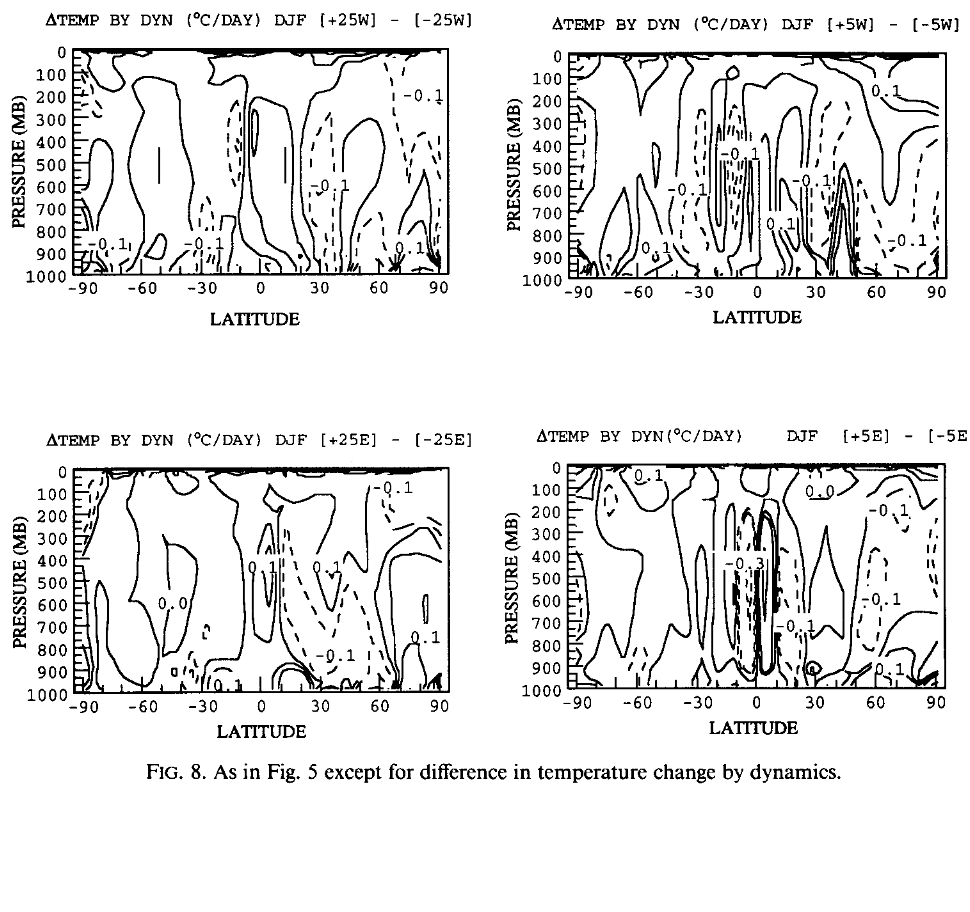

FIG. 8. As in Fig. 5 except for difference in temperature change by dynamics.

change is associated with the dynamical temperature forcing.

Differences also exist at low latitudes. In contrast to the QBO experiments, here the tendency is for warming of the lower stratosphere associated with increased UV, and hence an increase in stability and a decrease in the Hadley circulation and total cloud cover. Once again the exception is the [+5W] − [−5W] experiments where the opposite effects occur. The model responses for the different experiments are given in Table 2.

4. Combined effect of UV variations and the QBO

In addition to a postulated dependence of tropospheric phenomena on the QBO and solar cycle, the LvL observations also imply a higher-order effect, that is, that the solar max minus solar min influence is different when combined with the west phase of the QBO than with the east phase, in both the stratosphere and troposphere. Off hand, this would not seem qualitatively implausible in the stratosphere, since the altered refraction characteristics associated with different vertical shear of the zonal wind (UV effect) would be operating on wave energy whose horizontal refraction pattern has already been affected by an altered horizontal shear of the zonal wind (QBO effect). Similarly, if differences occur in the stratosphere, they could have an impact on the troposphere by altering the vertical stability. The separation of solar influence by QBO phase is the unique aspect of the Labitzke-van Loon studies.

We have already seen that the model does show such differences, at least with the exaggerated UV forcing employed; in this section we portray the effects more directly. We compare the temperature change between [+25W minus −25W] and [+25E minus −25E], and between [+5W minus −5W] and [+5E minus −5E] in Fig. 9. The increased UV warms the polar lower stratosphere more in the W experiments than in the E experiments. [Coincidentally or not, as noted in Part I, this is in agreement with the LvL observations that stratospheric warmings are more common in the maximum phase of the solar cycle during the west wind QBO phase, although as can be seen in Fig. 5, the model produces *warmer* temperatures in this region during the west wind phase only with the more realistic (5%) UV forcing.] In response, the extratropical troposphere cools more in the W experiments.

The mechanisms behind this difference are those described in Part I: the altered refraction characteristics of the atmosphere, with increased UV an increase in the vertical wind shear, are favoring vertical propagation of planetary wave energy from the polar lower stratosphere to higher levels, producing a net E–P flux divergence in the polar lower stratosphere. In all the QBO experiments, there is greater planetary wave propagation to higher latitudes in the lower stratosphere during the east phase, but with increased UV energy, upward propagation is favored largely poleward of 65° latitude, while with decreased UV it is favored largely equatorward of 65° latitude (and thus discouraged at higher latitudes). Thus, the gain of energy in the high-latitude lower stratosphere during the E phase of the QBO preferentially propagates vertically out of the polar lower stratosphere region when the UV is at a maximum, and, therefore, its warming effect is minimized. This result is shown schematically in Fig. 10 for the east phase with +25 UV. With the smaller magnitude of UV forcing, the vertical shear of the zonal wind is not as great in the upper stratosphere, wave propagation is less favorable to high levels and more favorable at lower levels, hence the effect on the lower stratospheric QBO is enhanced.

The differences are thus summarized as follows, where "+UV" and "−UV" can represent the 25% or 5% changes:

1) more poleward propagation in E than W experiments;

2) with +UV, upward propagation at high latitudes away from lower stratosphere;

3) thus, less increase in wave energy convergence in the polar lower stratosphere for E–W during +UV phase: +UV, E polar lower stratosphere "not as warm" (as −UV, E), +UV, W polar stratosphere "not as cold" (as −UV, W);

4) in −UV phase, vertical propagation in poleward region is discouraged, relative poleward energy flux in E phase thus stays in lower stratosphere: −UV, E polar stratosphere is "warm," −UV, W polar stratosphere is "cold";

5) then 3)–4) implies [+UV, W minus −UV, W] is equivalent to ["not as cold" minus "cold"] = "warming";

6) and [+UV, E minus −UV, E] is equivalent to ["not as warm" minus "warm"] = "cooling";

7) then, finally, 5)–6) implies [+UV, W minus −UV, W] − [+UV, E minus −UV, E] is equivalent to warming–cooling, hence a warmer lower stratosphere with increased UV in the west phase of the QBO than in the east phase (Fig. 10). With reduced propagation to higher altitudes, the polar region in the upper stratosphere and lower mesosphere is relatively cooler.

The situation at midlatitudes can be explained in precisely the reverse fashion. Now vertical propagation is inhibited in the +UV experiments, and thus, the gain from the QBO E phase is greater; this imposes the reverse tendency to that indicated for the pole, suggesting cooling for this region as the conclusion given in statement 7), with warming above, in the middle and upper stratosphere. The latitudinal variation of the response is clearly shown in Fig. 9.

What does this imply for the troposphere? In the polar regions where the lower stratosphere/upper troposphere warming is large, there is as expected reduced eddy energy and reduced tropospheric energy trans-

TABLE 2. Northern Hemisphere tropospheric (1000–200 mb) changes in UV experiments, for the months of December through February.

	Parameter			
	[+25E minus −25E]	[+25W minus −25W]	[+5E minus −5E]	[+5W minus −5W]
Δtemperature(°C) (60°–90°N)	0.7	0.2	0.2	−1.5
Δstatic stability (%) (60°–90°N)	−7.4	−3.0	−2.3	6.8
ΔEKE (%) (50°–80°N)	2.0	4.0	3.9	−5.5
Δnorthward eddy transport of energy (%) (NH)	5.5	2.3	4	−7.2
Δtemperature (68 mb) (10°S–15°N)	1.5	1.1	0.4	−0.4
ΔHadley cell (%)	−5.2	−4.2	−1.2	3.0
Δcloud cover (absolute %) (10°S–15°N)	−3.3	−2.9	0.6	2.7

ports (see Table 3). This promotes a general cooling tendency, with a dynamical energy divergence of some 5 W m^{-2}. Additional temperature responses are associated with changes in tropospheric radiative conditions: in colder regions there is more snow cover, increasing the albedo, and cloud cover changes arise associated with the change in eddy energy. At the highest latitudes, the warmer polar stratosphere is radiating more energy down to the surface, promoting warming (seen most clearly in the 25% runs).

The decreased temperatures in the tropical lower stratosphere reduce low-latitude tropical stability, and induce a tendency for tropospheric Hadley cell circulation increases. However, this increase is confined to the tropical locations; in the subtropics where the lower stratosphere warms, the tropospheric Hadley circulation decreases in intensity. Cloud cover changes arise in response to this dynamical variation as well.

The results shown in Table 3 indicate that the differing effects of the UV forcing between the two phases of the QBO are sharpened by using the more realistic (5%) variations. In most cases the effects were seen

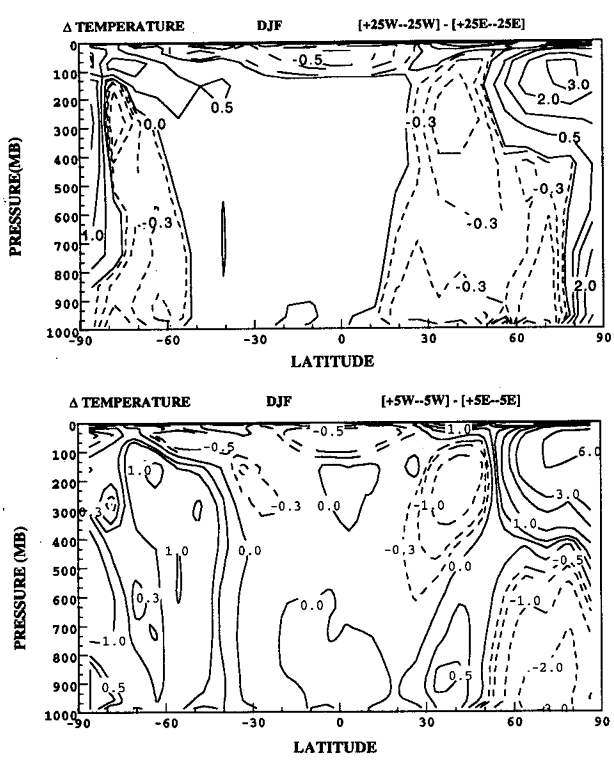

FIG. 9. Composite average model temperature difference (°C) for December through February between increased and reduced UV experiments for each phase of the QBO: {[+25W minus −25W] minus [+25E minus −25E]} (top); and {[+5W minus −5W] minus [+5E minus −5E]} (bottom).

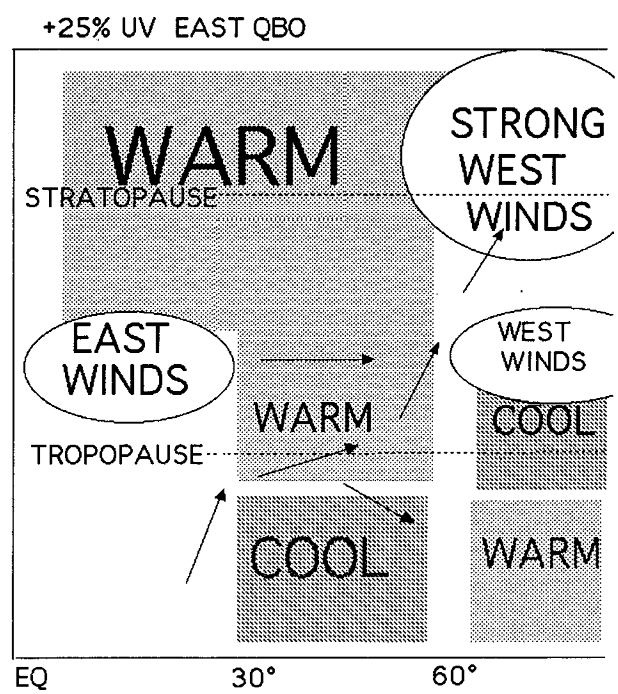

FIG. 10. Schematic of middle atmosphere/troposphere response to QBO and altered UV. The example given is for changes due to the east phase of the QBO with increased solar UV. Tropical east winds lead to greater poleward propagation of planetary wave energy (arrows) in the lower stratosphere, producing warming at midlatitudes. The increased UV produces general warming at low to midlatitudes, and increased west winds at higher levels in the extratropics. This larger vertical shear of the zonal wind is associated with greater upward planetary wave energy propagation, taking energy out of the polar lower stratosphere, which thus cools. The extratropical tropospheric response is opposite to that of the lower stratosphere, due to the effects of changes in vertical stability on eddy energy and high cloud cover.

TABLE 3. Northern Hemisphere tropospheric changes in combined QBO/UV experiments, for the months of December through February.

	Parameter	
	(+25 W minus −25W) minus [+25E minus −25E]	(+5W minus − 5W) minus [+5E minus −5E]
Δtemperature (°C) (60°–90°N)	−0.5	−1.3
Δstatic stability (%) (60°–90°N)	4.0	9.1
ΔEKE (%) (50°–80°N)	2.0	−9.4
Δnorthward eddy transport of energy (%) (NH)	−3.3	−11.2
Δtemperature (68 mb) (10°S–15°N)	−0.4	0.8
ΔHadley cell (%)	1.0	4.2
Δcloud cover (absolute %) (10°S–15°N)	0.4	1.9

with 25% forcing as well, but the localization of the wave energy propagation impact to the lower stratosphere, which occurs with the smaller UV forcing, amplifies the changes.

5. Longitudinal responses

a. *Modeled response to UV/QBO variations*

One of the most intriguing aspects of the Labitzke–van Loon analysis concerns the particular longitudinal responses apparently associated with the different phases of the solar/QBO variations. In exploring the model results, the question of longitudinal response must be considered within the framework of the experimental format. In all of these experiments the sea surface temperatures have not been allowed to change. This is probably of somewhat lesser consequence for the QBO experiments, as the short timescale of the phenomena would likely preclude much of any thermodynamic oceanic response (although ocean dynamical responses are of course possible). Nevertheless, limiting the oceanic response does influence the surface level by impacting land/ocean temperature gradients. For example, in [E–W], the ground temperature cooling at midlatitudes over land is up to 1°C (averaged over the 3 years of the run), in contrast to the lack of change possible for the ocean surface, and the surface *air* temperature response over land is ten times larger than over the oceans. This difference is greater than would be expected from the actual QBO, which would last only 1 year in the east or west phase (and at a constantly changing altitude and amplitude), although some difference in response over land versus ocean would likely occur. Note further, that allowing a terrestrial surface response but not allowing sea surface temperatures to change is not responsible for the decrease in extratropical eddy energy. If anything, cooling the land relative to the ocean should increase the normal winter land versus ocean contrast, and increase eddy energy, as occurred in model experiments with ice age condition contrasts (Rind 1987).

The inability of the sea surface temperatures to respond is potentially of somewhat greater consequence for the altered UV experiments, although the magnitude of the problem is uncertain. With solar cycle variations lasting for up to 5–6 years (one-half the solar cycle) some cumulative response for the oceans might be expected; however, the QBO itself would be continually changing phase during this period, perhaps interrupting any consistent geographic pattern of response. An analysis of the correlation of sea surface temperature changes with the solar cycle for the last decade does indicate regions of significant correlation (Y. Tsubota 1995, personal communication), although it does not necessarily imply a causal connection.

Within this general limitation, shown in Fig. 11 are the surface air temperature changes for [+25W minus −25W], [+25E minus −25E] [+5W minus −5W], and [+5E minus −5E]. The translation of the zonal average temperature changes given in Fig. 5 to the longitudinal response can be understood by comparing these two figures. In all sets of experiments that show a cooling in the lower stratosphere ([+25E minus −25E], [+25W minus −25W], [+5E minus −5E]) a primary region of consistency is the warming over Eurasia north of 60°N, with cooling farther south. As the region with the largest land concentration, this area is primarily responsible for the inverse correlation between lower stratosphere and lower troposphere temperature changes seen in Fig. 5. In the one set of experiments in which there is warming in the lower stratosphere ([+5W minus −5W]), the surface temperature pattern reverses, with cooling north of 60°N, and warming farther south. Similar differences occur in the 700-mb height field (Fig. 12), with ridging in association with warming, and other tropospheric patterns [e.g., jet stream winds, as have been related to solar cycle variations by John (1989), and storm tracks by Tinsley (1988)].

The responses are associated with changes in standing planetary wave amplitude and phase. Shown in Fig. 13a,b are the amplitude and phase changes of standing wavenumber 1 in these runs. All the sets of experiments that show cooling in the lower stratosphere have an increase in wavenumber 1 amplitude of sizable proportion relative to the control throughout the troposphere, switching to a decrease in the stratosphere. The phase of this wave shifts westward in these exper-

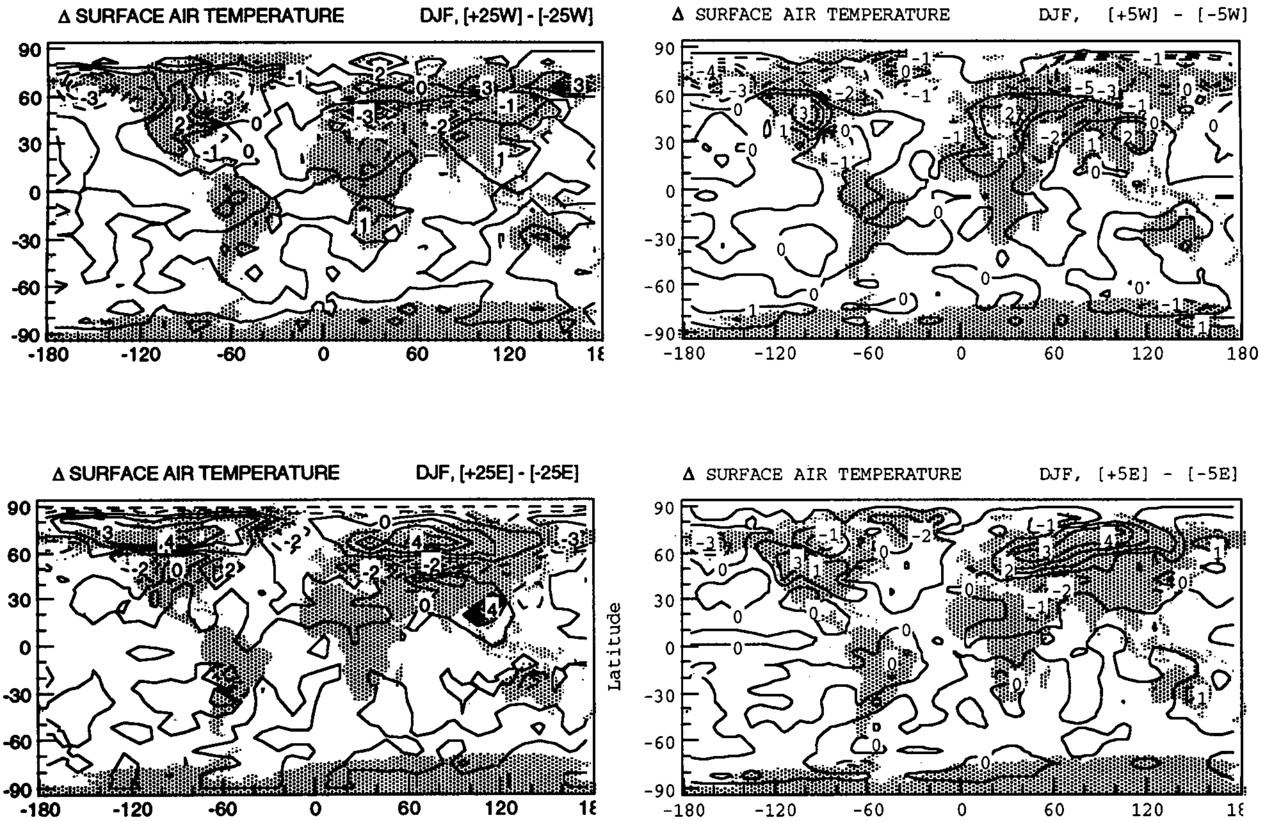

FIG. 11. Composite average model surface air temperature difference (°C) for December through February between UV extremes: [+25W minus −25W] (upper left); [+25E minus −25E] (bottom left); [+5W minus −5W] (upper right); and [+5E minus −5E] (lower right).

iments. In contrast, in the {[+5W] − [−5W]} set, which had warming in the lower stratosphere, the wave amplitude decreases in the lower troposphere, and the phase shifts eastward. (The 10% UV experiments, which produced warming in the lower stratosphere, also had this response.) Note this result is consistent with the conclusion from Part I of greater dependence on the phase of the QBO with the more realistic UV forcing.

Kodera (1994) noted that a change in wave energy propagation is consistent with an alteration in the ridge/trough pattern. As was shown in Part I (Fig. 11), the three runs that produce similar wavenumber 1 responses all display an upward/equatorward wave energy flux change in the troposphere from 60°–90°N, while {[+5W] − [−5W]} has a downward/poleward energy flux change. Alterations in both wave generation and propagation are responsible.

The geographic variation in temperature for the UV extremes between the two phases of the QBO are given in Fig. 14. The high latitude tropospheric cooling visible in the zonal average picture (Fig. 9) is clearly displayed over the land areas. Once again the general magnitudes are somewhat larger with the reduced UV forcing, as was the lower stratospheric warming.

b. Robustness of results

As noted in Part I, results from just 3 years of these experiments may be expected to be influenced by the model's natural variability. To explore this issue, we compare the 3-year averages with results from the full 10 years of the 5% experiments. A suitable summary is provided by the surface air temperature changes between the [+5] and [−5] experiments in both the west and east phases, and their difference (Fig. 11, right; Fig. 14, bottom). The 10-year average results are given in Fig. 15. The primary features displayed in Figs. 11 and 14 are all reproduced: cooling at high latitudes in the west wind phase, warming in the east wind phase, and thus large differences between UV maximum and minimum in the two different phases. The result is not surprising, given the similarity in stratospheric response between the 3-year and 10-year results (Part I, Fig. 13), but it does verify the consistency of the stratospheric/tropospheric coupling discussed above.

c. Comparison with observations

Given the limitations of the experiments vis-à-vis real world forcing and potential ocean response, the

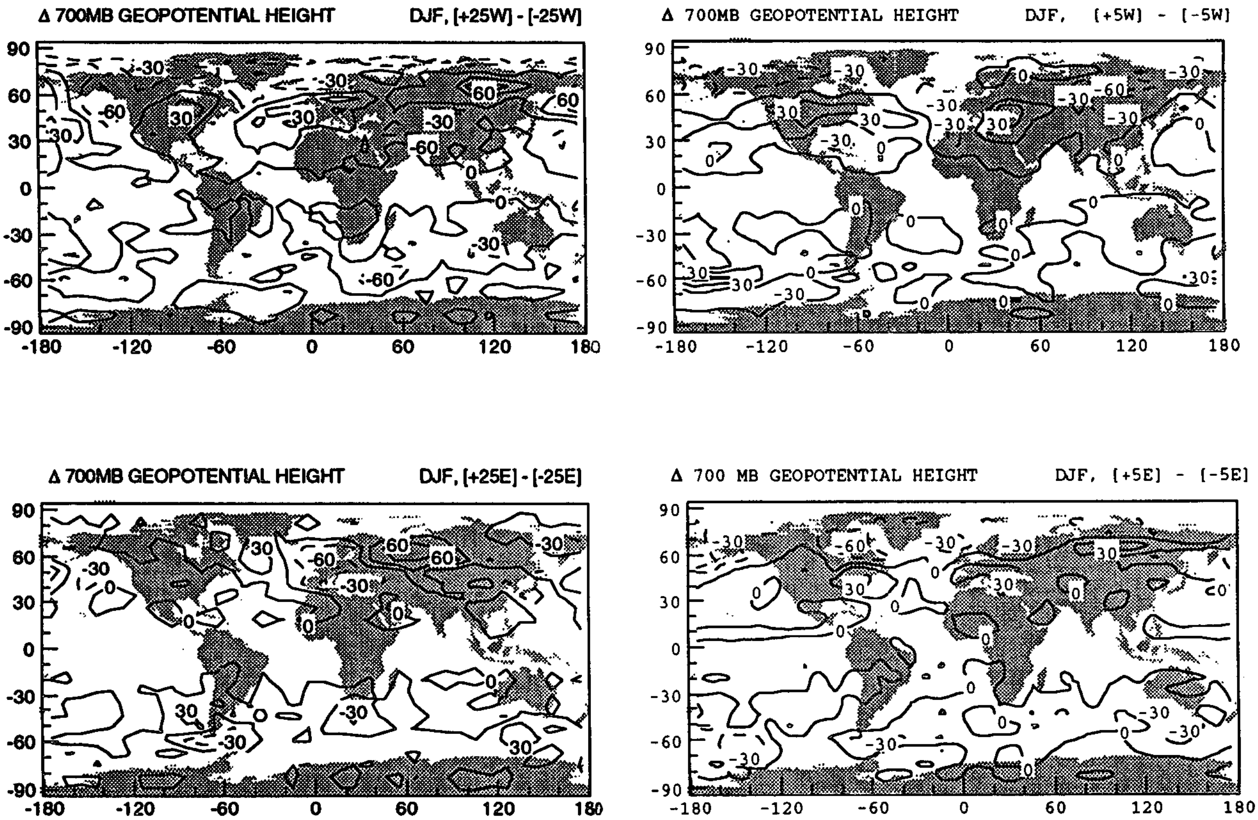

FIG. 12. As in Fig. 11 except for difference (in meters) of 700-mb geopotential heights.

purpose of this comparison is primarily to assess how the relative patterns and magnitudes of the effects found here compare with those that the LvL studies have suggested arise from combined solar UV/QBO forcing. We focus on the 5% experiments, which produced the more realistic stratospheric response, but as emphasized in Part I (Fig. 14), even this magnitude is an exaggeration of the likely solar forcing. The outstanding feature in the model is that with increased UV, northern Eurasia cools during the west phase, and warms during the east phase (Fig. 15), with the differences peaking around 70°N (Fig. 15). (For this comparison we use the full 10-year averages.) In general, van Loon and Labitzke (1988) found similar results, although their peak changes were about 30°E of those shown in Fig. 15. Farther south over Eurasia (30°–40°N) the observations indicated the reverse effect, with increased UV warming during the west phase and cooling during the east phase. As can be seen in Fig. 15, the model shows a similar tendency, though with longitudinal variability.

Over North America, the observations show that with increased UV, colder temperatures generally prevail poleward of 70°N, while warmer conditions occur between 45° and 70°N; model results are more or less in agreement. South of 45°N observations indicate cooling conditions, while the model shows little change. Given the deviation of the experiment from the real world forcing, and the uncertainty as to whether the observed effects are really solar UV-related, any agreement might be viewed as simply coincidental. However, the high-latitude stratospheric responses in the experiments were similar to observations, so the tropospheric responses might be expected to be as well, and the regions of greatest agreement are those that feature high-latitude tropospheric cooling below the regions of stratospheric warming.

Quantitatively, the LvL observations indicate that the magnitude of the apparent solar flux variations in surface air temperature are on the order of 5°C. Model results are of a similar or slightly smaller magnitude.

The 700-mb anomalies in the model generally match those found in observations where the surface temperature anomalies are similar. The height variations amount to generally one-half to two-thirds of the reported values.

6. Discussion and conclusions

The primary results of these experiments are as follows (results pertain to Northern Hemisphere in winter):

1) As the QBO east phase produces warming in the extratropical lower stratosphere/upper troposphere, cooling occurs below in the troposphere. The high-level warming increases tropospheric static stability, reduces

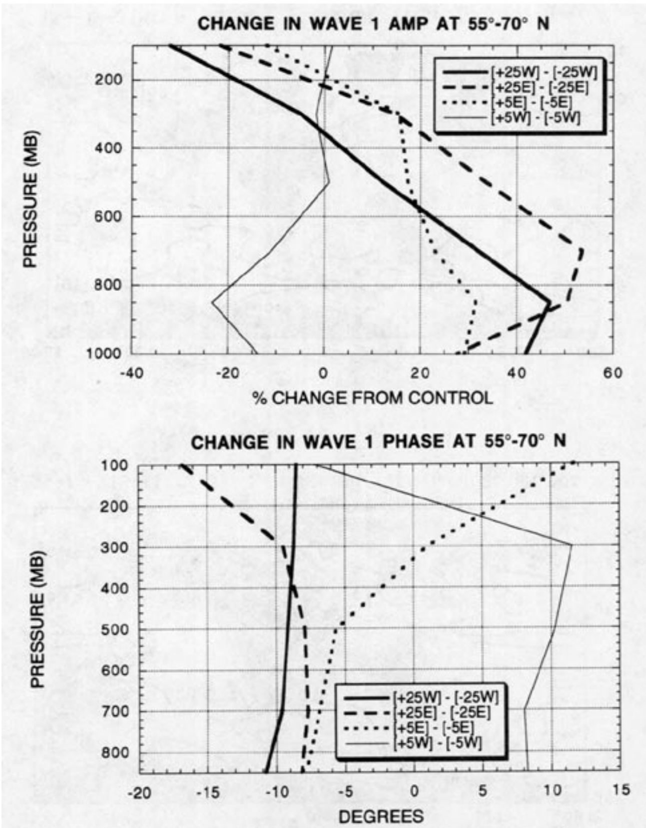

FIG. 13. Change in standing wave 1 properties in December through February averaged over 55°–70°N: (a) amplitude as a percentage of the control run average; (b) phase.

eddy energy and eddy transports, hence producing the cooling below. With more realistic UV forcing, differences begin to appear between UV max and UV min experiments. With reduced UV, effects peak at higher latitudes than with increased UV.

2) With increased UV, the high-latitude lower stratosphere/upper troposphere cools in most experiments, and the troposphere below warms. The high-level cooling reduces the vertical stability, resulting in increased eddy energy, increased eddy transports, and dynamic warming. The one exception is the [+5W] − [−5W] experiment in which the opposite effects arise: warming in the high-latitude lower stratosphere/upper troposphere, and cooling in the troposphere below. This distinction in polar stratospheric response between the phases of the QBO in the 5% experiments is in agreement with observations.

3) Due to their effects on planetary wave generation and propagation, all combinations of UV and QBO phases affect the longitudinal patterns of tropospheric temperatures and heights. The nature of the perturbations is often qualitatively consistent with the observations, and of similar or slightly smaller magnitude. Surface temperature responses of up to 5°C occur, with 700-mb height variations of up to 60 m, while variations of standing wavenumber 1 amplitude reach 40% in the lower troposphere. For both the UV and QBO experiments, zonal average tropospheric dynamical changes are on the order of 5%. The results thus show that local changes on the order of those ascribed to solar variability can result from small percentage alterations in tropospheric processes, some of which are probably below the level of accurate observations.

4) Dynamical changes also arise at low latitudes, associated with changes in vertical stability and the Hadley circulation. Effects are again on the order of 5%.

As discussed in Part I, these experiments cannot in themselves prove that the LvL observations are accurately ascribing tropospheric variations to solar influence. Even the ±5% variations are larger than may be occurring at 0.3 μm and if the real world effects are being driven by stratospheric zonal wind variations of 20–50 m s^{-1}, as some observations imply, those cannot be obtained in these experiments with realistic UV variations. As in Part I, however, the model reproduces many of the observed effects with the more realistic UV changes without correspondingly large wind variations, primarily because it does not require large vari-

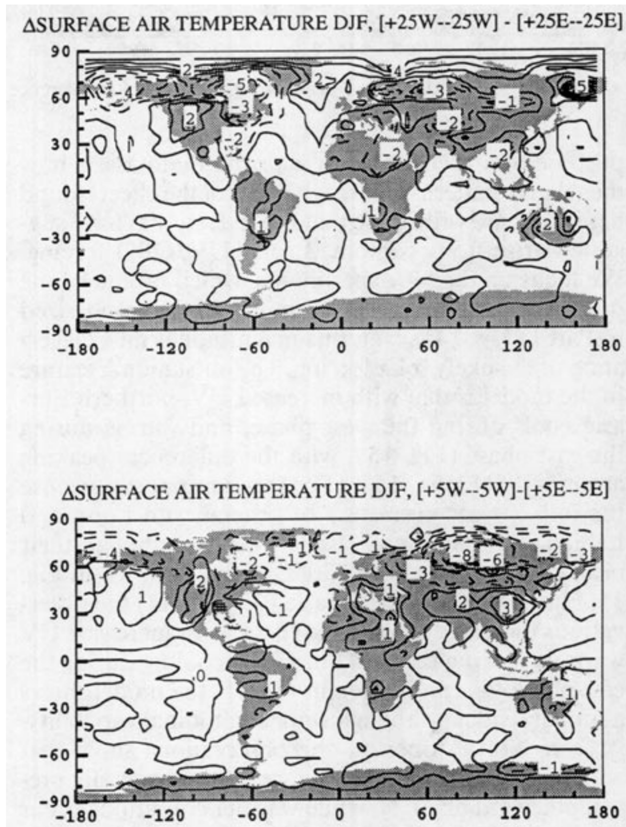

FIG. 14. Composite average model surface air temperature difference (°C) for December through February for {[+25W minus −25W] minus [+25E minus −25E]} (top); and {[+5W minus −5W] minus [+5E minus −5E]} (bottom).

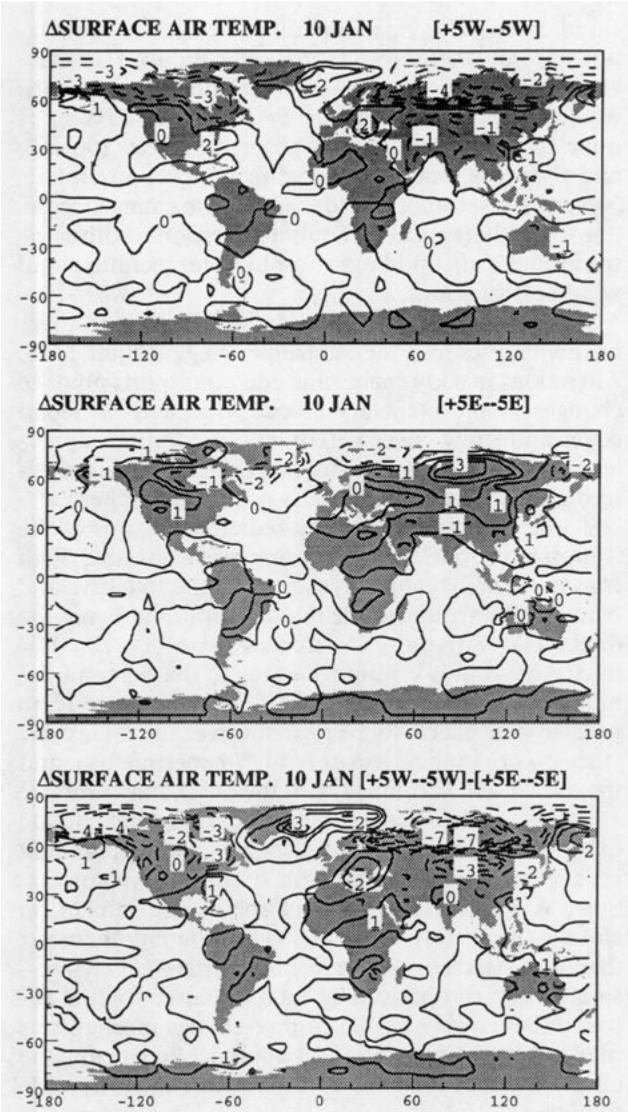

FIG. 15. Model surface air temperature difference (°C) averaged over 10 Januarys for [+5W] minus [−5W] (top), [+5E] minus [−5E] (middle); and [+5W minus −5W] minus [+5E minus 5E] (bottom).

ations in total energy to reproduce some of the observations.

Therefore, the major contribution of this work is to delineate a possible causal connection between solar UV/QBO cycles and the Labitzke–van Loon observations of middle atmospheric and tropospheric variability. The results suggest that mechanisms do exist within the system to produce appropriate patterns and magnitudes of change to UV forcing, but whether the actual UV forcing is sufficiently large (or the system sufficiently sensitive) is still undetermined. (It may be noticed that Fig. 14 in Part I shows that the UV variations employed in the 5% runs are of the same order of magnitude as the available observations.) The essence of this connecting link is the ability of the longest tropospheric planetary waves to respond to perturbations in the stratosphere. This is a consistent response in the GISS model when the stratosphere is fully resolved, an effect which is strong enough to result in increased planetary wavenumber 1 energy in the doubled CO_2 climate simulations (due to the colder stratosphere reducing the vertical stability), even while the decrease in the tropospheric latitudinal temperature gradient was resulting in an overall decrease in tropospheric eddy kinetic energy (Rind et al. 1990).

The suggestion of planetary wave involvement in the UV/QBO connection is not new (e.g., Ebel et al. 1988), and there are observations from the middle atmosphere of in-phase and out-of-phase apparent solar cycle correlations as a function of altitude, which imply the involvement of waves of large vertical wavelength (e.g., Chanin et al. 1989). The longest planetary waves have vertical wavelengths varying from 15 to 100 km or more (Charney and Drazin 1961), and conceptually, should be able to respond to perturbations affecting a significant part of their vertical structure.

There are two components to the planetary wave response: a propagation change and a generation change. The propagation change depends upon alterations in the stratospheric wind profiles. The QBO impacts the stratospheric zonal wind structure by changing the horizontal gradient, and recent observations imply that the solar cycle is effective in changing the vertical gradient. While the modeled variations in wind with more realistic UV forcing are smaller than those found by Kodera and Yamazaki (1990) or Hood et al. (1993), some variation is to be expected given the change in latitudinal heating gradient from ozone absorption of the changing UV (see Table 4b in Part I).

The change in planetary wave generation is associated with temperature changes in the upper troposphere through the stratosphere, altering the vertical stability for the longest planetary waves. The most relevant temperature changes are dynamically produced, through alterations in zonal winds, planetary wave energy convergences, and the residual circulation. This is accomplished directly in the low to middle stratosphere via the QBO forcing, and in the middle and upper stratosphere by the UV variations; UV-induced temperature changes in the lower stratosphere then occur in response to altered planetary wave propagation.

Two-dimensional photochemical models have predicted only a modest change of stratospheric temperature due to 11-year solar cycle UV variations, on the order of 1°C at 50 km (Garcia et al. 1984; Huang and Brassuer 1993), as the large percentage variations in solar cycle UV occur for energy absorbed above the stratopause. In contrast, observations imply much larger effects (up to 5°C in the stratosphere) at a wide range of latitudes (Mohanakumar 1989; Chanin and Keckhut 1991; Hood et al. 1993). A similar discrepancy exists between 1D model results and observations of the 27-day solar rotational cycle effects (Brassuer et al. 1987; Hood and Jirikowic 1991).

A primary limitation of the 1D and 2D approaches is that dynamical feedbacks are not available to amplify initial perturbations. This is true not only of the UV forcing itself; the combined processes of the QBO and UV variations produce nonlinear dynamical responses. To some extent, the UV effects may be looked upon as modulations of the QBO, an influence which would not be modeled if the QBO were not also included in the study.

Changes in ozone and molecular oxygen may induce additional radiative perturbations; Hood et al. (1993) show that changes in ozone observed during the last solar cycle are somewhat larger than 2D model estimates of direct solar cycle influence, and they suggest alterations in circulation as the likely reason. In the model experiments, residual circulation changes do accompany UV/QBO perturbations. For example, in the QBO experiments during December through February, the lower stratosphere Northern Hemisphere residual circulation increased by more than 50%, while the Southern Hemisphere subtropical circulation actually changed direction (both effects due to increased planetary wave energy convergence at high latitudes). In the tropical upper stratosphere, the residual circulation decreased by 50%, due to the altered gravity wave drag. In the UV experiments, the changes were less dramatic, with variations of the lower stratospheric residual circulation during December through February of about 15% in each hemisphere, while in the middle and upper stratosphere, increases of this magnitude occur in the Tropics and Northern Hemisphere (due to planetary wave energy propagating preferentially to higher altitudes). As emphasized by Chanin and Keckhut (1991), fully coupled 3D dynamical–photochemical models of the middle atmosphere may be necessary to resolve these issues, along with continuing observational analysis.

Variations of tropospheric eddy energy associated with solar phenomena have been noted on even shorter timescales. Roberts and Olson (1973) found that the vorticity area index of tropospheric storms was correlated to solar geomagnetic storms with a few day lag, and Wilcox et al. (1974) related a similar tropospheric feature to solar wind magnetic sector crossings. Tinsley (Tinsley and Deen 1991; Tinsley and Heelis 1993) suggests that cosmic ray and electric field impacts on ice nucleation in the upper troposphere could be providing these effects, with alterations in latent heat release affecting storm dynamics. While there is no necessity for any one physical phenomena to account for all possible effects, to the extent that solar energetic particle emissions impart heating to the middle atmosphere, changes in vertical stability could affect planetary wave generation on short timescales as well.

The dynamic responses in the model included alterations in the Hadley circulation, and, therefore, cloud cover. This raises an additional issue, the relationship of these results to solar-induced climate changes. Even in the $\pm 25\%$ UV variations experiments, which amounted to an energy change of 2 W m^{-2}, none of that alteration was absorbed below 100 mb, and, therefore, would have no direct impact on climate. Nevertheless, tropospheric temperature changes arose, due to the dynamical and radiative response within the troposphere to middle atmosphere temperature and wind perturbations.

Changes in the Hadley circulation affect cloud cover in the Tropics and the subtropics (e.g., Tables 1–3). Alterations in eddy energy and eddy transports produce changes in the planetary albedo, due both to cloud cover and snow cover variations. In addition, upper-level clouds are affected by eddy energy changes, altering the greenhouse capacity of the atmosphere.

These effects influence the radiative balance of the troposphere, but the alterations are associated with tropospheric dynamical responses to the radiative and dynamical warming of the middle atmosphere, not the direct UV variation. Differences arise between UV maximum and UV minimum due to the different dynamical/radiative feedbacks. In addition, there is no necessity for effects to average out over the solar cycle (they do not in these exaggered UV experiments), and the cycle itself, combined with the QBO, may produce a net forcing. Were a cycling sun to have a net climate forcing when averaged over the entire cycle, this could be a repeating influence with a cumulative impact. Since it would be an indirect solar cycle impact on climate, it is likely to have a very different character than that associated with greenhouse trace gas changes, so a simple comparison of total radiative forcing between these two potential climate change mechanisms may not be the most relevant approach to gauging the effectiveness of solar variability relative to greenhouse forcing.

From both dynamic and climatic considerations, future experiments should employ the proper magnitude/wavelengths of solar irradiance variations (including the visible and near IR component). Ozone changes associated with the solar cycle should be included as well, especially if they are as large and occurring at the range of altitudes suggested by the observations of Hood et al. (1993). The model should ideally have the proper planetary long wave energy, to allow the absolute magnitude of change to be accurately calculated (most climate models underestimate the longest planetary wave energy by up to 50%). The sea surface temperatures and sea ice should be allowed to adjust, to amplify the climate perturbations during each phase of the UV/QBO oscillation, and for determining the impact when averaged over the solar cycle. And instead of simply using extremes, the full solar cycle, and transitional nature of the QBO should be employed, to include the nonlinear effects that arise with intermediate forcing. Only with such complete experiments will we be able to assess whether the (modeled) system has sufficient sensitivity to respond to the proposed forcing mechanisms.

Acknowledgments. We thank Patrick Lonergan for his help in setting up model experiments and providing diagnostic output of the results. Alan Plumb helped design the QBO experiments and some model diagnostics, and Judith Lean provided advice concerning solar UV variations. This work was supported by NSF Grant ATM9208266, while the model development work has been funded by the NASA Upper Atmosphere Program Office.

REFERENCES

Barnston, A. G., and R. E. Livezey, 1989: A closer look at the effect of the 11-year solar cycle and the quasi-biennial oscillation in the Northern Hemisphere 700 mb height and extratropical North American surface temperature. *J. Climate,* **2,** 1295–1313.

Boville, B. A., 1984: The influence of the polar night jet on the tropospheric circulation in a GCM. *J. Atmos. Sci.,* **41,** 1132–1142.

——, 1993: The stratosphere in general circulation models. *The Role of the Stratosphere in Global Change,* M.-L. Chanin, Ed., Springer-Verlag, 199–214.

Brasseur, G., A. De Rudder, G. M. Keating, and M. C. Pitts, 1987: Response of the middle atmosphere to short-term solar ultraviolet variation. Part II: Theory. *J. Geophys. Res.,* **92,** 903–914.

Chanin, M. L., and P. Keckhut, 1991: Influence on the middle atmosphere of the 27-day and 11-year solar cycles: Radiative and/or dynamical forcing? *J. Geomag. Geoelectr.,* **43**(Suppl.), 647–655.

——, ——, A. Hauchecorne, and K. Labitzke, 1989: The solar activity, QBO effect in the lower thermosphere. *Ann. Geophys.,* **7,** 463–470.

Charney, J. G., and P. G. Drazin, 1961: Propagation of planetary scale disturbances from the lower into the upper atmosphere. *J. Geophys. Res.,* **66,** 83–109.

Ebel, A., M. Dameris, and H. J. Jakobs, 1988: Modeling of the dynamical response of the middle atmosphere to weak external forcing: Influence of stationary and transient waves. *Ann. Geophys.,* **6,** 501–512.

Friis-Christensen, E., and K. Lassen, 1991: Length of the solar cycle: An indicator of solar activity closely associated with climate. *Science,* **254,** 698–700.

Garcia, R., S. Solomon, R. G. Roble, and D. W. Rush, 1984: Numerical response of the middle atmosphere to the 11-year solar cycle. *Planet. Space Sci.,* **32,** 411–423.

Hood, L. L., and J. J. Jirikowic, 1991: Stratospheric dynamical effects of solar ultraviolet variations: Evidence from zonal mean ozone and temperature data. *J. Geophys. Res.,* **96,** 7565–7577.

——, and D. Zaff, 1995: Lower stratospheric stationary waves and the longitude dependence of ozone trends in winter. *J. Geophys. Res.,* in press.

——, J. L. Jirikowic, and J. P. McCormack, 1993: Quasi-decadal variability of the stratosphere: Influence of long-term solar ultraviolet variations. *J. Atmos. Sci.,* **50,** 3941–3958.

Huang, T. Y. W., and G. Brasseur, 1993: Effect of long-term solar variability in a two-dimensional interactive model of the middle atmosphere. *J. Geophys. Res.,* **98,** 20 413–20 427.

John, J. I., 1989: Storm tracks and atmospheric circulation indices over the northeast Atlantic and northwest Europe in relation to the solar cycle and the QBO. *Proc. Workshop on Mechanisms for Tropospheric Effects of Solar Variability and the Quasi-biennial Oscillation,* S. K. Avery and B. A. Tinsley, Eds., Boulder, CO, National Science Foundation/CEDAR and SLOSTEP, 209–219.

Kodera, K., 1993: Influence of the stratospheric circulation change on the troposphere in the Northern Hemisphere winter. *The Role of the Stratosphere in Global Change,* M.-L. Chanin, Ed., Springer-Verlag, 199–214.

——, 1994: Influence of volcanic eruptions on the troposphere through stratospheric dynamical process in the Northern Hemisphere winter. *J. Geophys. Res.,* **99,** 1273–1282.

——, and K. Yamazaki, 1990: Long-term variation of upper stratospheric circulation in the Northern Hemisphere in December. *J. Meteor. Soc. Japan,* **68,** 101–105.

——, and ——, 1994: A possible influence of polar stratospheric coolings on the troposphere in the Northern Hemisphere winter. *Geophys. Res. Lett.,* **21,** 809–812.

——, ——, M. Chiba, and K. Shibata, 1990: Downward propagation of upper stratospheric mean zonal wind perturbation to the troposphere. *Geophys. Res. Lett.,* **17,** 1263–1266.

Labitzke, K., and H. van Loon, 1988: Association between the 11-yr solar cycle, the QBO and the atmosphere. Part I: The troposphere and stratosphere in the Northern Hemisphere in winter. *J. Atmos. Terr. Phys.,* **50,** 197–206.

——, and ——, 1989: Association between the 11-yr solar cycle, the QBO and the atmosphere. Part III: Aspects of the association. *J. Climate,* **2,** 554–565.

Mohanakumar, K., 1989: Influence of solar activity on middle atmosphere associated with phases of equatorial QBO. *MAP Handbook,* **29,** 39–42.

Rind, D., 1987: Components of the ice age circulation. *J. Geophys. Res.,* **92,** 4241–4281.

——, R. Suozzo, N. K. Balachandran, A. Lacis, and G. Russell, 1988a: The GISS global climate/middle atmosphere model. Part I: Model structure and climatology. *J. Atmos. Sci.,* **45,** 329–370.

——, ——, and ——, 1988b. The GISS global climate/middle atmosphere model. Part II: Model variability due to interactions between planetary waves, the mean circulation and gravity wave drag. *J. Atmos. Sci.,* **45,** 371–386.

——, ——, ——, and M. P. Prather, 1990: Climate change and the middle atmosphere. Part I: The doubled CO_2 climate. *J. Atmos. Sci.,* **47,** 475–494.

——, N. K. Balachandran, and R. Suozzo, 1992: Climate change and the middle atmosphere. Part II: The impact of volcanic aerosols. *J. Climate,* **5,** 189–208.

Roberts, W. O., and R. H. Olson, 1973: Geomagnetic storms and wintertime 300 mb trough development in the North Pacific–North America area. *J. Atmos. Sci.,* **30,** 135–140.

Tinsley, B. A., 1988: The solar cycle and QBO influence on the latitude of storm tracks in the North Atlantic. *Geophys. Res. Lett.,* **15,** 409–412.

——, and G. W. Deen, 1991: Apparent tropospheric response to MeV-GeV particle flux variations: A connection via electrofreezing of supercooled water in high-level clouds? *J. Geophys. Res.,* **96,** 22 283–22 296.

——, and R. A. Heelis, 1993: Correlations of atmospheric dynamics with solar activity. Evidence for a connection via the solar wind, atmospheric electricity, and cloud microphysics. *J. Geophys. Res.,* **98,** 10 375–10 384.

van Loon, H., and K. Labitzke, 1988: Association between the 11-yr solar cycle, the QBO and the atmosphere. Part II: Surface and 700 mb in the Northern Hemisphere in winter. *J. Climate,* **1,** 905–920.

Wilcox, J. M., P. H. Scherrer, L. Svalgaard, W. O. Roberts, R. H. Olson, and R. L. Jenne, 1974: Influence of solar magnetic structure on terrestrial atmospheric vorticity. *J. Atmos. Sci.,* **31,** 581–588.